

Planetary boundary layer and atmospheric turbulence.

Szymon P. Malinowski

Institute of Geophysics UW

2018/19

Lecture 06



Phenomenology of the Atmospheric Boundary Layer (PBL).

In classical fluid dynamics, a **boundary layer is the layer in a nearly inviscid fluid next to a surface in which frictional drag associated with that surface is significant** (term introduced by Prandtl, 1905).

Such boundary layers can be laminar or turbulent, and are often only mm thick.

In atmospheric science, a similar definition is useful. The **atmospheric boundary layer (ABL, sometimes called P[lanetary] BL) is the layer of fluid directly above the Earth's surface in which significant fluxes of momentum, heat and/or moisture are carried by turbulent motions whose horizontal and vertical scales are on the order of the boundary layer depth, and whose circulation timescale is a few hours or less** (Garratt, p. 1). A similar definition works for the ocean.

The complexity of this definition is due to several complications compared to classical aerodynamics.

- i) Surface heat exchange can lead to thermal convection
- ii) Moisture and effects on convection
- iii) Earth's rotation
- iv) Complex surface characteristics and topography.

BL is assumed to encompass surface-driven dry convection. Most workers (but not all) include shallow cumulus in BL, but deep precipitating cumuli are usually excluded from scope of BLM due to longer time for most air to recirculate back from clouds into contact with surface.

BLM also traditionally includes the study of fluxes of heat, moisture and momentum between the atmosphere and the underlying surface, and how to characterize surfaces so as to predict these fluxes (roughness, thermal and moisture fluxes, radiative characteristics). Includes plant canopies as well as water, ice, snow, bare ground, etc.

PBL characteristics

The boundary layer itself exhibits dynamically distinct sublayers:

- i) Interfacial sublayer - in which molecular viscosity/diffusivity dominate vertical fluxes
- ii) Inertial layer - in which turbulent fluid motions dominate the vertical fluxes, but the dominant scales of motion are still much less than the boundary layer depth.

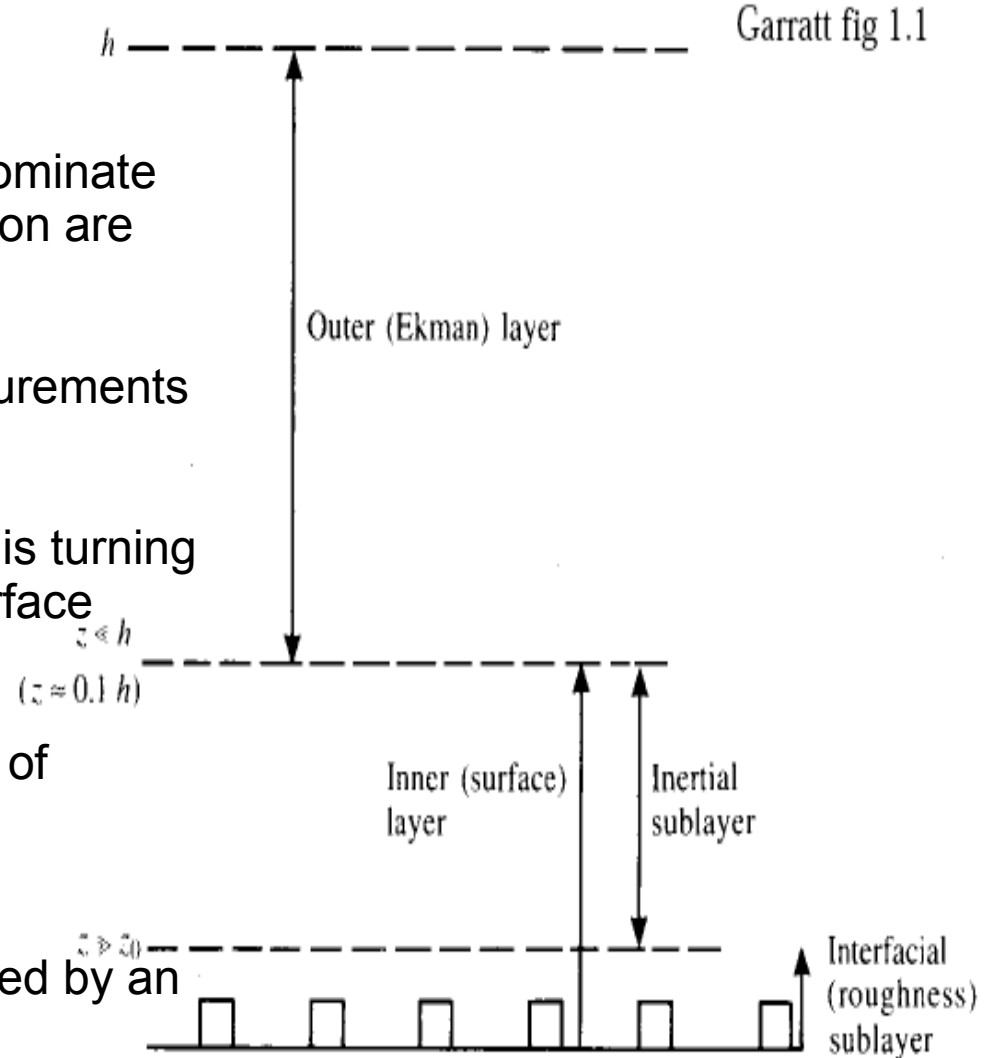
This is the layer in which most surface wind measurements are made.

- Layers (i) + (ii) comprise the surface layer. Coriolis turning of the wind with height is not evident within the surface layer.

- iii) Outer layer - turbulent fluid motions with scales of motion comparable to the boundary layer depth ('large eddies').

- At the top of the outer layer, the BL is often capped by an entrainment zone in which turbulent BL eddies are entraining non-turbulent free-atmospheric air. This entrainment zone is often associated with a stable layer or inversion.

- For boundary layers topped by shallow cumulus, the outer layer is subdivided further into subcloud, transition, cumulus and inversion layer.



PBL meteorology- applications.

The boundary layer is the part of the atmosphere in which we live and carry out most human activities. Furthermore, almost all exchange of heat, moisture, momentum, naturally occurring particles,

aerosols, and gasses, and pollutants occurs through the BL. Specific applications:

- i) Climate simulation and NWP - parametrization of surface characteristics, air-surface exchange, BL thermodynamics fluxes and friction, and cloud. No climate model can succeed without some consideration of the boundary layer. In NWP models, a good boundary layer is critical to proper prediction of the diurnal cycle, of low-level winds and convergence, of effects of complex terrain, and of timing and location of convection. Coupling of atmospheric models to ocean, ice, land-surface models occurs through BL processes.
- ii) Air Pollution and Urban Meteorology - Pollutant dispersal, interaction of BL with mesoscale circulations. Urban heat island effects.
- iii) Agricultural meteorology - Prediction of frost, dew, evapotranspiration.
- iv) Aviation - Prediction of fog formation and dissipation, dangerous wind-shear conditions.
- v) Remote Sensing - Satellite-based measurements of surface winds, skin temperature, etc. Involve the interaction of BL and surface, and must often be interpreted in light of a BL model to be useful for NWP.

PBL equations – Boussinesq approximation

For simplicity, we will use the Boussinesq approximation to the Navier-Stokes equations to describe boundary-layer flows. This is quite accurate for the ABL (and ocean BLs as well), since:

1. The ABL depth $O(1 \text{ km})$ is much less than the density scale height $O(10 \text{ km})$.
2. Typical fluid velocities are $O(1-10 \text{ ms}^{-1})$, much less than the sound speed.

The Boussinesq equations of motion are:

$$\frac{D\mathbf{u}}{Dt} + f\mathbf{k} \times \mathbf{u} = -\frac{\nabla p'}{\rho_0} + b\mathbf{k} + [\nu \nabla^2 \mathbf{u}], \text{ where buoyancy } b = g\theta_v/\theta_0$$

$$\nabla \cdot \mathbf{u} = 0$$

$$\frac{D\theta}{Dt} = S_\theta + [\kappa \nabla^2 \theta], \quad S_\theta \approx -\frac{1}{\rho_0 C_p} \frac{\partial R_N}{\partial z} \text{ in the absence of clouds}$$

$$\frac{Dq}{Dt} = S_q + [\kappa_q \nabla^2 q], \quad S_q = 0 \text{ in the absence of precipitation}$$

Here p' is a pressure perturbation, θ is potential temperature, $q = q_v + q_l$ is mixing ratio (including water vapor q_v and liquid water q_l if present), and $\theta_v = \theta(1 + .608q_v - q_l)$ is virtual potential temperature including liquid water loading. S denotes source/sink terms, and ρ_0 and θ_0 are characteristic ABL density and potential temperature. κ and κ_q are the diffusivities of heat and water vapor. The most important source term for θ is divergence of the net radiative flux R_N (usually treated as horizontally uniform on the scale of the boundary layer, though this needn't be exactly true, especially when clouds are present). For noprécipitating BLs, $S_q = 0$. For cloud-topped boundary layers, condensation, precipitation and evaporation can also be important.

Using mass continuity, the substantial derivative of any quantity a can be written in flux form 5

$$Da/Dt = \partial a / \partial t + \nabla \cdot (\mathbf{u}a).$$

The ensemble average of Da/Dt is:

$$\begin{aligned} \overline{\frac{Da}{Dt}} &= \overline{\frac{\partial a}{\partial t}} + \nabla \cdot \overline{\mathbf{u}a} \\ &= \frac{\partial}{\partial t} \bar{a} + \frac{\partial}{\partial t} \overline{a'} + \frac{\partial}{\partial x} \overline{(\bar{u} + u')(a + a')} + \frac{\partial}{\partial y} \overline{(\bar{v} + v')(a + a')} + \frac{\partial}{\partial z} \overline{(\bar{w} + w')(a + a')} \\ &= \frac{\partial}{\partial t} \bar{a} + \nabla \cdot \bar{\mathbf{u}} \bar{a} + \frac{\partial}{\partial x} \overline{u' a'} + \frac{\partial}{\partial y} \overline{v' a'} + \frac{\partial}{\partial z} \overline{w' a'} \end{aligned}$$

The three **eddy correlation** terms at the end of the equation express the net effect of the turbulence. Consider a BL of characteristic depth H over a nearly horizontally homogeneous surface. The most energetic turbulent eddies in the boundary layer have horizontal and vertical lengthscale H and (by mass continuity) the same scale U for turbulent velocity perturbations in both the horizontal and vertical. The boundary layer structure, and hence the eddy correlations, will vary horizontally on characteristic scales $L_s \gg H$ due to the impact on the BL of mesoscale and synoptic-scale variability in the free troposphere. If we let $\{\}$ denote ‘the scale of’, and assume $\{a'\} = A$, we see that **the vertical flux divergence is dominant**:

$$\left\{ \frac{\partial}{\partial x} \overline{u' a'} \right\} = \frac{UA}{L_s} \ll \left\{ \frac{\partial}{\partial z} \overline{w' a'} \right\} = \frac{UA}{H}$$

Thus (noting also that $\nabla \cdot \bar{\mathbf{u}} = 0$ to undo the flux form of the advection of the mean),

$$\overline{\frac{Da}{Dt}} \approx \frac{\partial}{\partial t} \bar{a} + \bar{\mathbf{u}} \cdot \nabla \bar{a} + \frac{\partial}{\partial z} \overline{w' a'}$$

If we apply this to the ensemble-averaged heat equation, and throw out horizontal derivatives of θ in the diffusion term using the same lengthscale argument $L_s \gg H$ as above, we find

$$\frac{\partial \bar{\theta}}{\partial t} + \bar{\mathbf{u}} \cdot \nabla \bar{\theta} = - \frac{\partial}{\partial z}(\overline{w'\theta'}) + \bar{S}_\theta + \left[\kappa \frac{\partial^2 \bar{\theta}}{\partial z^2} \right] \leftarrow \text{Can be neglected outside the surface layer}$$

Thus, the effect of turbulence on $\bar{\theta}$ is felt through the convergence of the vertical eddy correlation, or **turbulent flux** of θ . The turbulent **sensible and latent heat fluxes** are the turbulent fluxes of θ and q in energy units of W m^{-2} :

$$\text{Turbulent sensible heat flux} = \rho_0 C_p \overline{w'\theta'}$$

$$\text{Turbulent latent heat flux} = \rho_0 L \overline{w'q'}$$

Except in the interfacial layer within mm of the surface, the diffusion term is negligible, so we've written it in square brackets.



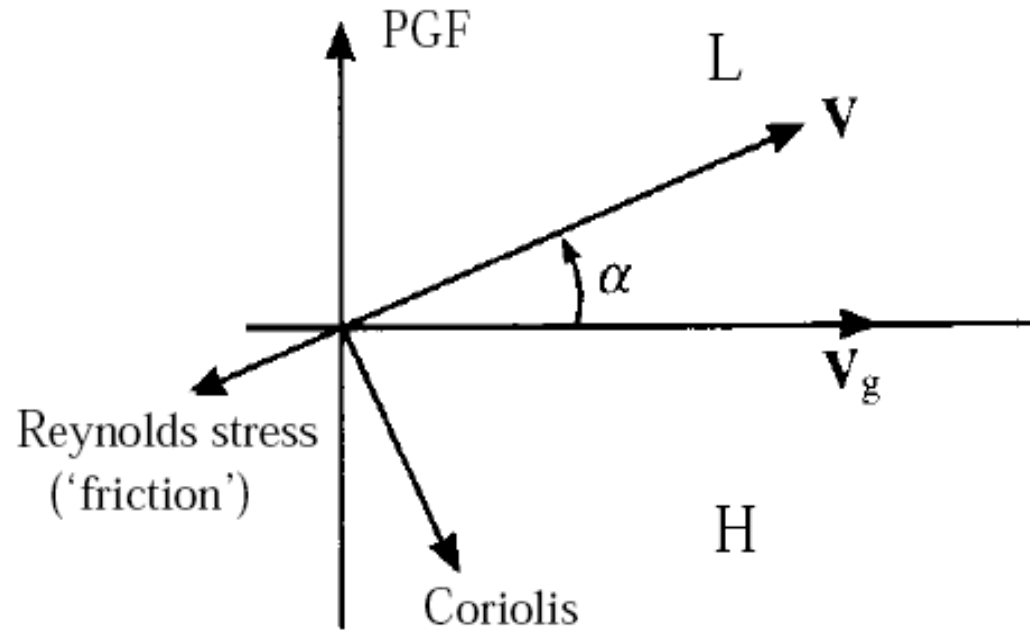
Rys. 3.2 Przykłady anemometrów akustycznych: ATI typ K o prostopadłych, nieprzecinających się osiach pomiarowych wykorzystywany do pomiarów przy ul. Lipowej (lewy rysunek) i R.M. Young 81000 o przecinających się osiach nieprostopadłych z umieszczoną obok głowicą analizatora gazowego Li-7500 (prawy rysunek).

If geostrophic wind u_g is defined in the standard way, the ensemble-averaged momentum equations are:

$$\frac{\partial \bar{u}}{\partial t} + \bar{\mathbf{u}} \cdot \nabla \bar{u} = f(\bar{v} - v_g) - \frac{\partial}{\partial z}(\overline{u'w'})$$

$$\frac{\partial \bar{v}}{\partial t} + \bar{\mathbf{u}} \cdot \nabla \bar{v} = -f(\bar{u} - u_g) - \frac{\partial}{\partial z}(\overline{v'w'})$$

Often, but not always, the tendency and advection terms are much smaller than the two terms on the right hand side, and there is an approximate three-way force balance between momentum flux convergence, Coriolis force and pressure gradient force in the ABL such that the mean wind has a component down the pressure gradient. The cross-isobar flow angle α is the angle between the actual surface wind and the geostrophic wind.



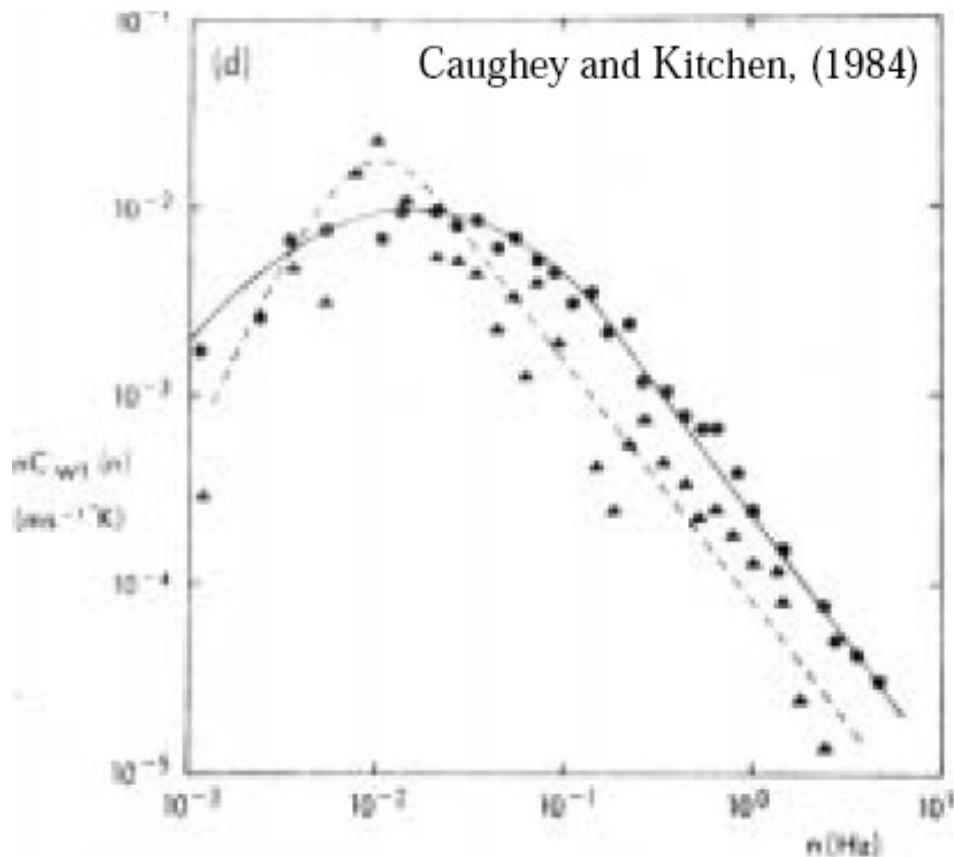
Surface layer force balance in a steady state BL ($f > 0$). Above the surface layer, the force balance is similar but the Reynolds stress need not be along $-V$.

If the mean profiles of actual and geostrophic velocity can be accurately measured, the momentum flux convergence can be calculated as a residual in the above equations, and vertically integrated to deduce momentum flux. This technique was commonly applied early in this century, before fast-response, high data rate measurements of turbulent velocity components were perfected. It was not very accurate, because small measurement errors in⁹ either u or u_g can lead to large relative errors in momentum flux.

In most BLs, the vertical fluxes of heat, moisture and momentum are primarily carried by large eddies with lengthscale comparable to the boundary layer depth, except near the surface where smaller eddies become important.

The figure below shows the cospectrum of w' and T' , which is the Fourier transform of $w'T'$, from tethered balloon measurements at two heights in the cloud-topped boundary layer we plotted in the previous lecture. The cospectrum is positive, i. e. positive correlation between w' and T' , at all frequencies, typical of a convective boundary layer.

Most of the covariance between w' and T' is at the same low frequencies $n = \omega/2\pi \sim 10^{-2}$ Hz that had the maximum energy. Since the BL is blowing by the tethered balloon at the mean wind speed $U = 7 \text{ ms}^{-1}$, this frequency corresponds to large eddies of wavelength $\lambda = U/n = 700 \text{ m}$, which is comparable to the BL depth of 1 km.



Cospectrum of w' and T' at cloud base (triangles), top (circles) in convective BL.

TKE equation in horizontally homogeneous PBL.

To form an equation for TKE $\bar{e} = \overline{\mathbf{u}' \cdot \mathbf{u}'}/2$, we dot \mathbf{u} into the momentum equation, and take the ensemble average. After considerable manipulation, we find that for the nearly horizontally homogeneous BL ($H \ll L_d$),

$$\frac{\partial}{\partial t} \bar{e} + \bar{\mathbf{u}} \cdot \nabla \bar{e} = S + B + T + D$$

where

$$S = -\overline{u'w'} \frac{\partial \bar{u}}{\partial z} - \overline{v'w'} \frac{\partial \bar{v}}{\partial z} \quad (\text{shear production})$$

$$B = \overline{w'b'} \quad (\text{buoyancy flux})$$

$$T = -\frac{\partial}{\partial z} \left(\overline{w'e'} + \frac{1}{\rho_0} \overline{w'p'} \right) \quad (\text{transport and pressure work})$$

$$D = -\overline{v|\nabla \times \mathbf{u}|^2} \quad (\text{dissipation, always negative, } -\epsilon \text{ in Garratt})$$

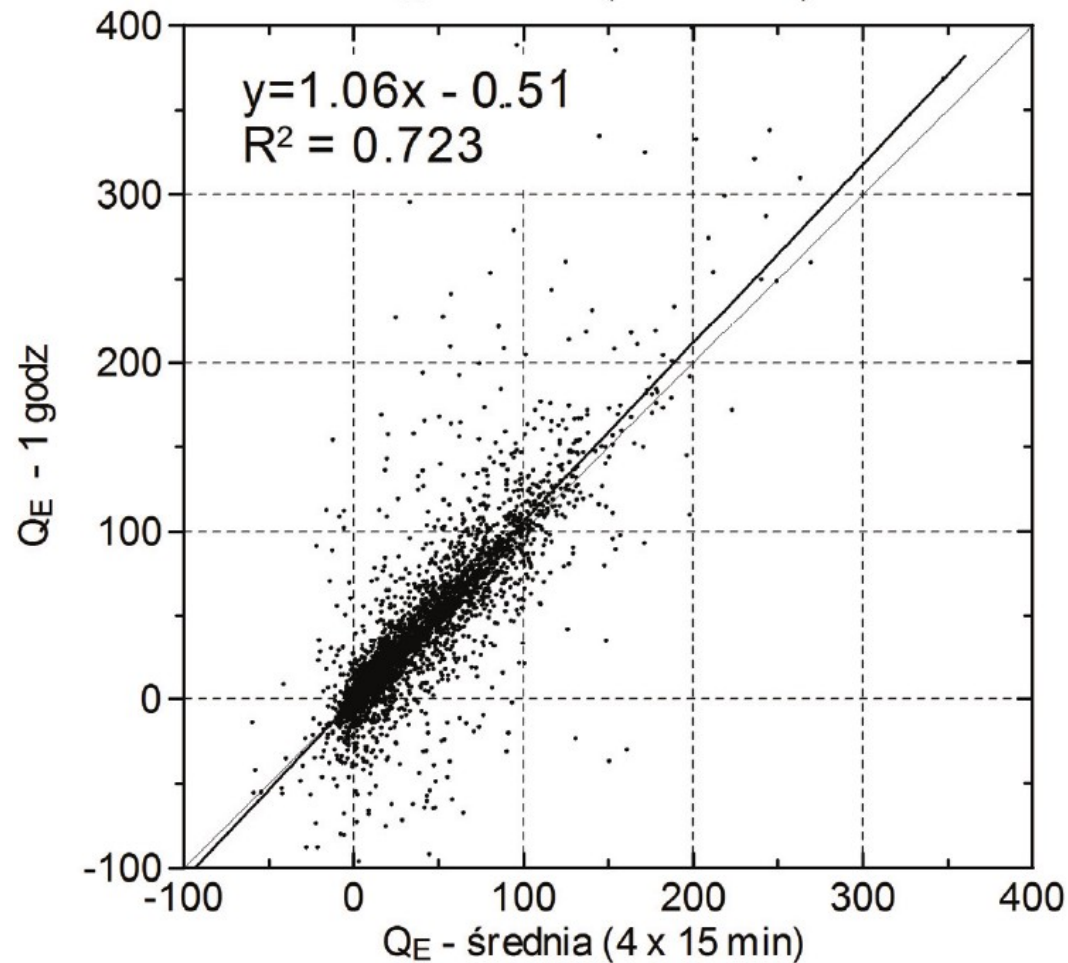
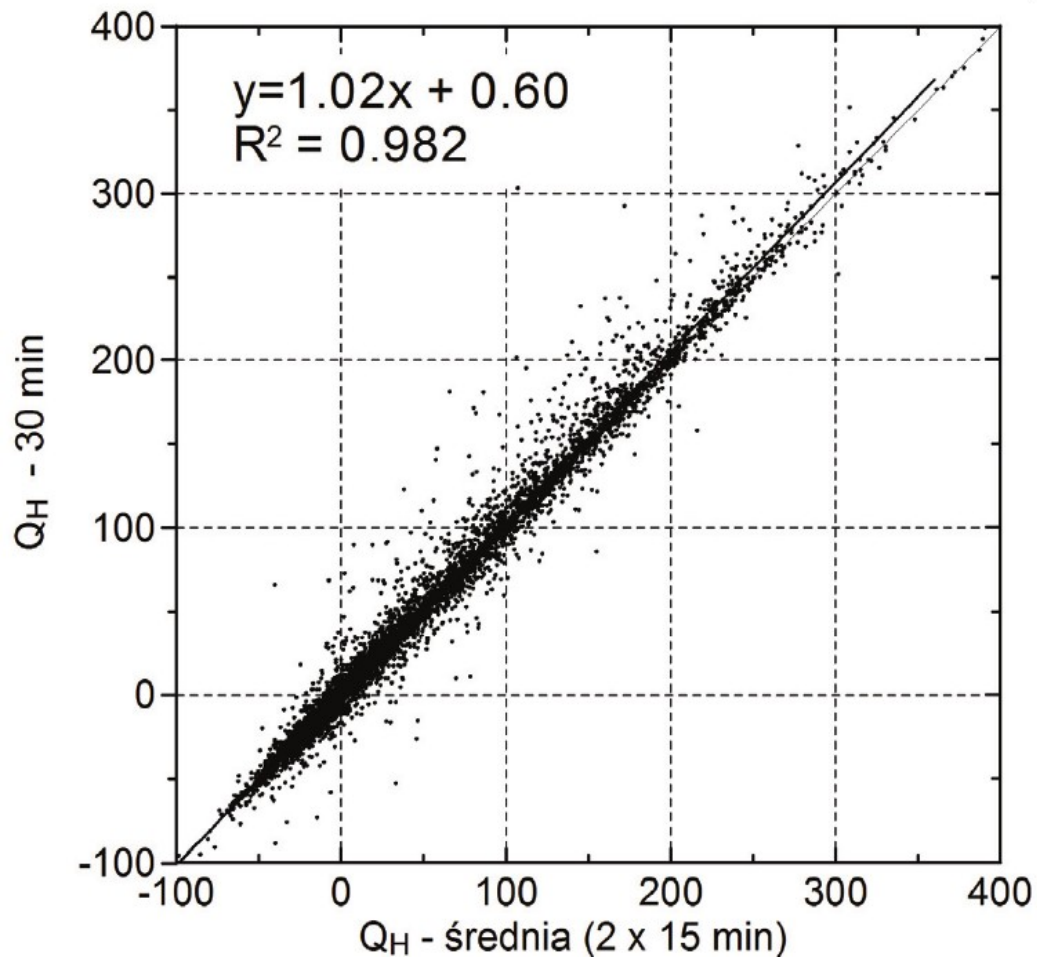
Shear production of TKE occurs when the momentum flux is downgradient, i. e. has a component opposite (or 'down') the mean vertical shear. To do this, the eddies must tilt into the shear. Kinetic energy of the mean flow is transferred into TKE.

Buoyancy production of TKE occurs where relatively buoyant air is moving upward and less buoyant air is moving downward. Gravitational potential energy of the mean state is converted to TKE.

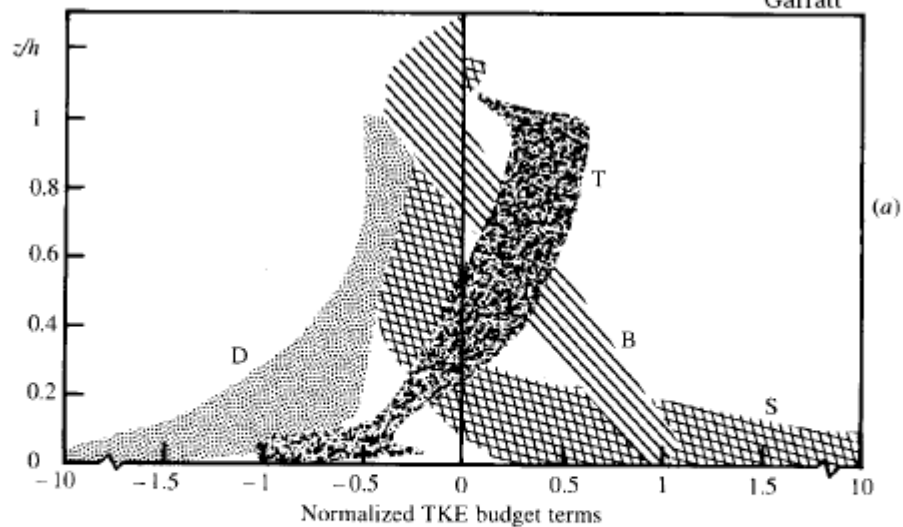
Both S and B can be negative at some or all levels in the BL, but together they are the main source of TKE, so the vertical integral of S + B over the BL is always positive.

The transport term mainly fluxes TKE between different levels, but a small fraction of TKE can be lost to upward-propagating internal gravity waves excited by turbulence perturbing the BL top.

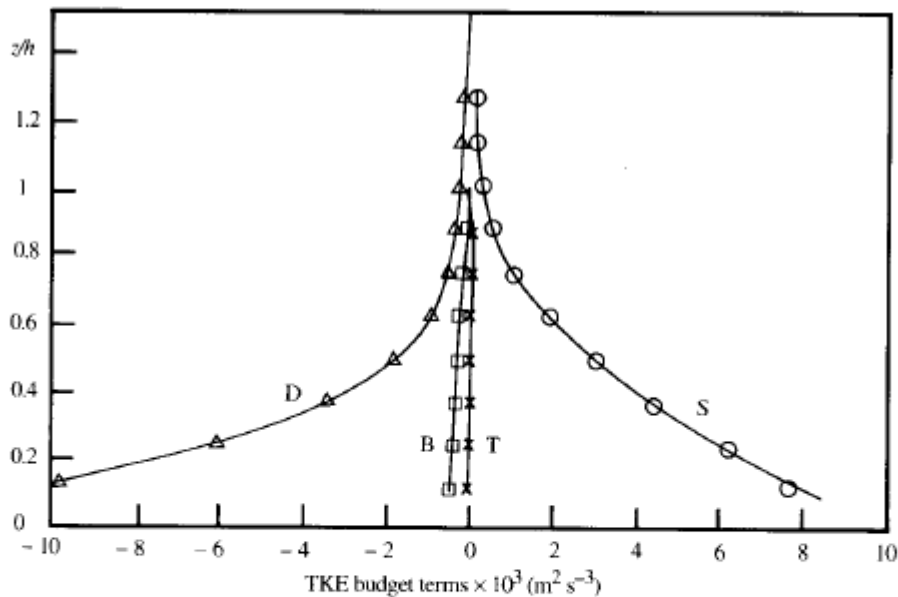
The dissipation term is the primary sink of TKE, and formally is related to enstrophy. In turbulent flows, the enstrophy is dominated by the smallest (dissipation) scales, so D can be considerable despite the smallness of n .



Comparison of turbulent latent heat fluxes estimated using 30 min (left) and 60 min (right) compared to corresponding 15 min averaging.



(a)



(b)

Fig. 2.4 Terms in the TKE equation (2.74b) as a function of height, normalized in the case of the clear daytime ABL (a) through division by w_*^3/h ; actual terms are shown in (b) for the clear night-time ABL. Profiles in (a) are based on observations and model simulations as described in Stull (1988; Figure 5.4), and in (b) are from Lenschow *et al.* (1988) based on one aircraft flight. In both, B is the buoyancy term, D is dissipation, S is shear generation and T is the transport term. Reprinted by permission of Kluwer Academic Publishers.

Usually, the left hand side (the 'storage' term) is smaller than the dominant terms on the right hand side.

The figure shows typical profiles of these terms for a daytime convectively driven boundary layer and a nighttime shear-driven boundary layer.

In the convective boundary layer, transport is considerable. Its main effect is to homogenizing TKE in the vertical .

With vertically fairly uniform TKE, dissipation is also uniform, except near the ground where it is enhanced by the surface drag . Shear production is important only near the ground (and sometimes at the boundary layer top).

In the shear-driven boundary layer, transport and buoyancy fluxes are small everywhere, and there is an approximate balance between shear production and dissipation. The flux Richardson number:

$$Ri_f = -B/S$$

characterizes whether the flow is stable ($Ri_f > 0$), neutral ($Ri_f \approx 0$), or unstable ($Ri_f < 0$).

TKE budget in stratocumulus topped marine boundary layer, LES of Kopec et al., 2016.

$$\frac{\partial \bar{e}}{\partial t} + \bar{w} \frac{\partial \bar{e}}{\partial z} = \frac{g}{\theta_v} \overline{w'\theta_v'} - \left(\overline{u'w'} \frac{\partial \bar{u}}{\partial z} + \overline{v'w'} \frac{\partial \bar{v}}{\partial z} \right) - \frac{\partial \bar{w'e}}{\partial z} - \frac{1}{\rho} \frac{\partial \bar{w'p'}}{\partial z} - \epsilon,$$

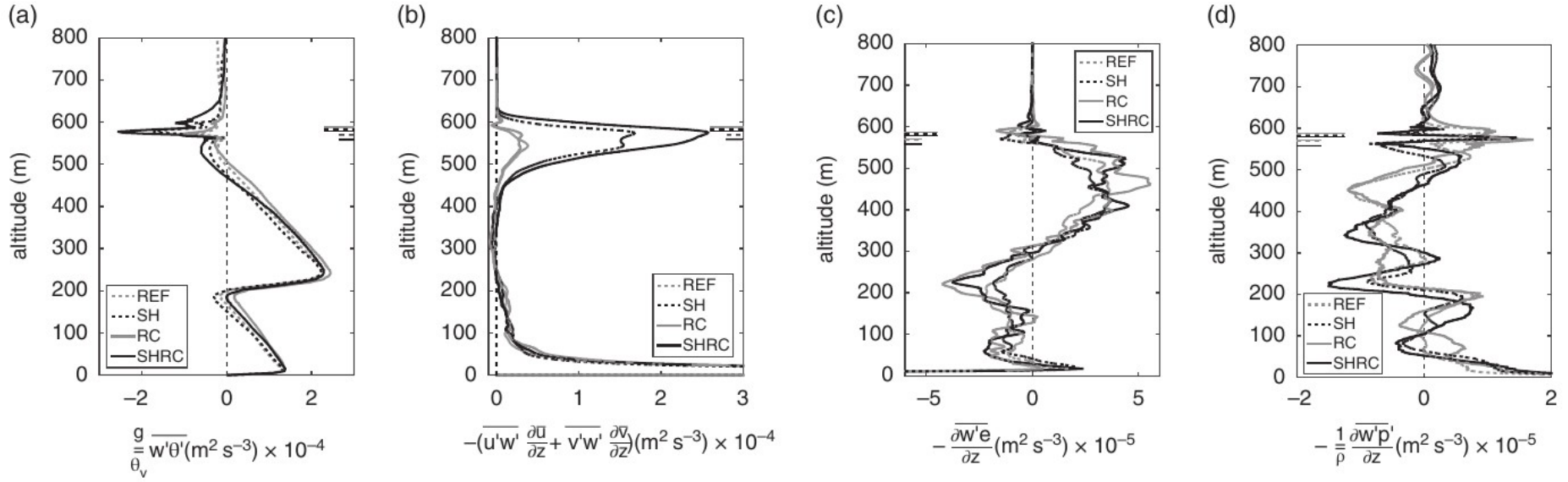


Figure 12. Time-averaged TKE budget terms (see abscissa description in panels a-d) calculated for the last hour of the simulations. Colour code as in Figure 4. Short horizontal lines indicate the cloud top and long horizontal lines mark the level of maximum gradient of liquid water potential temperature.

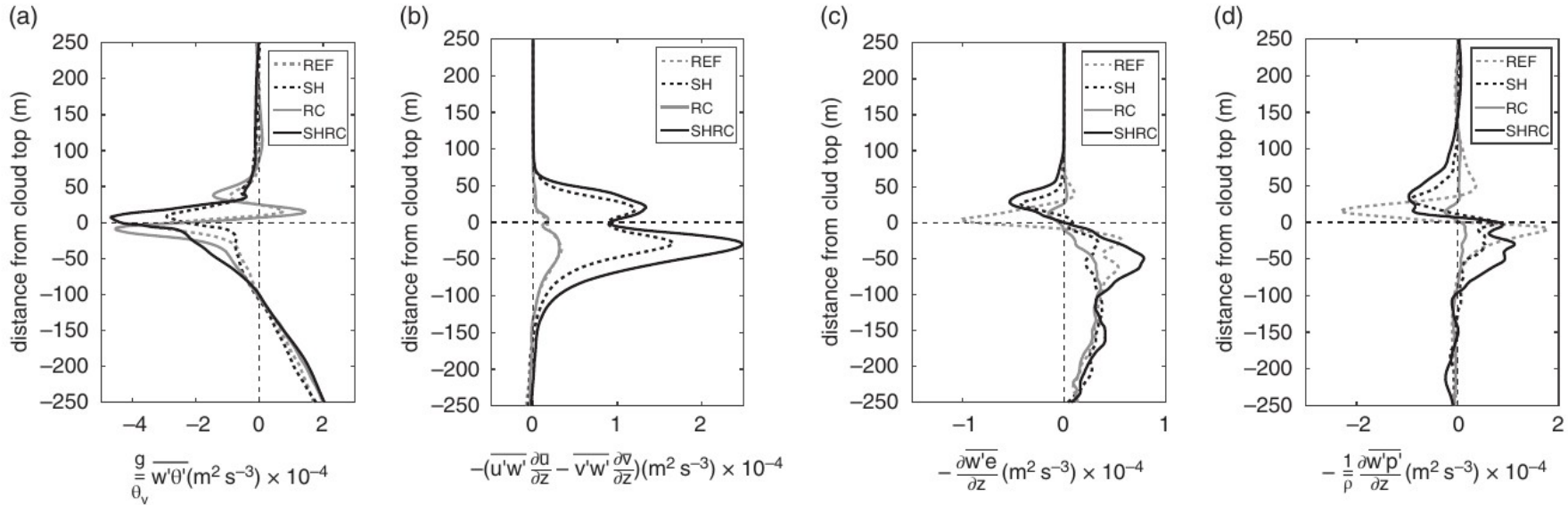
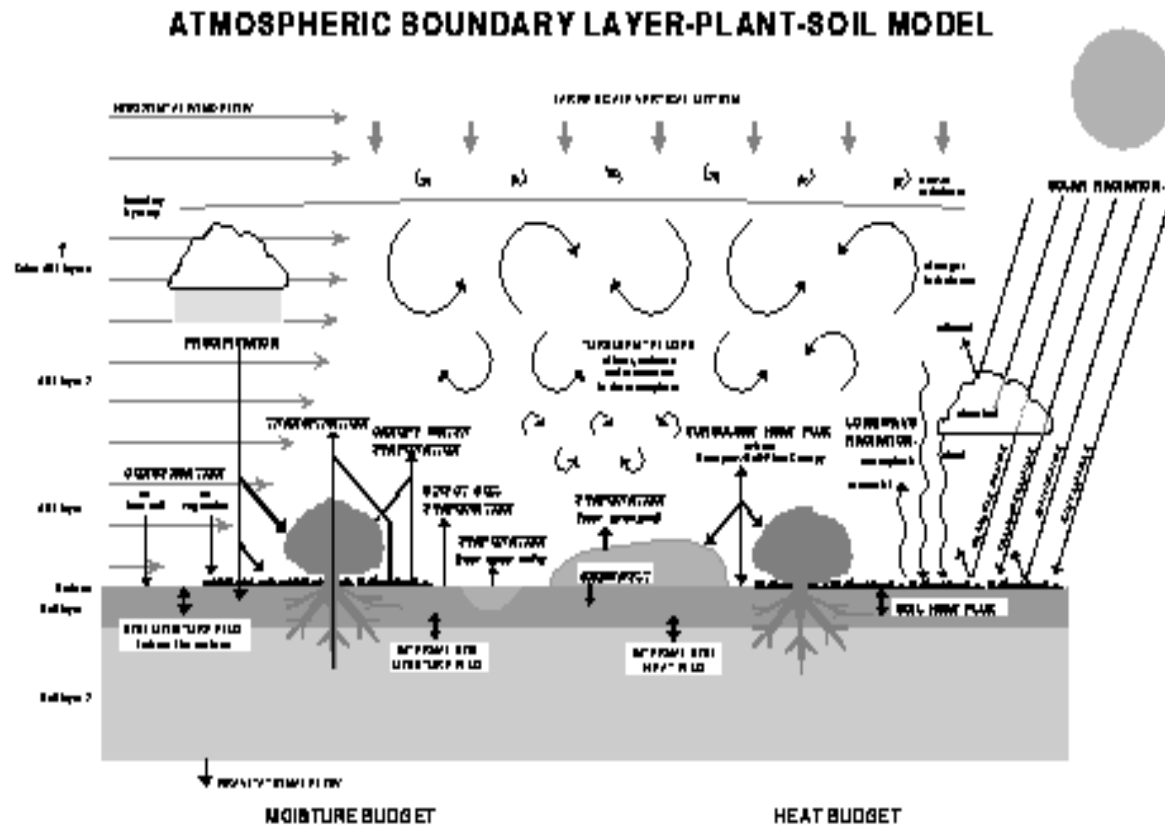
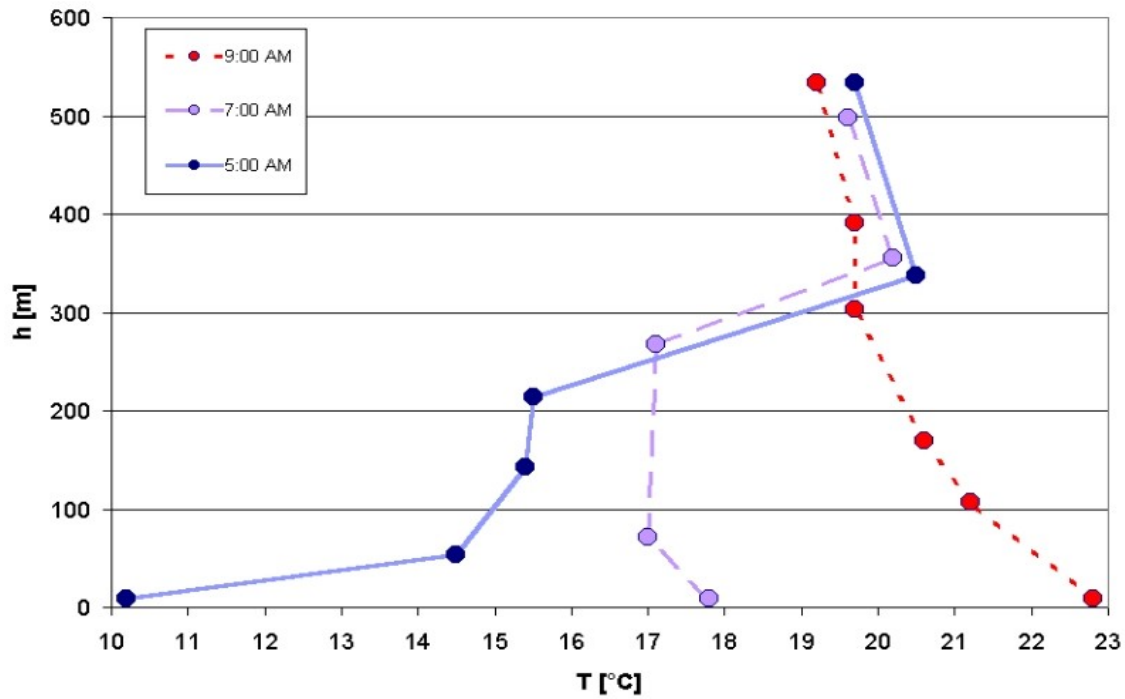


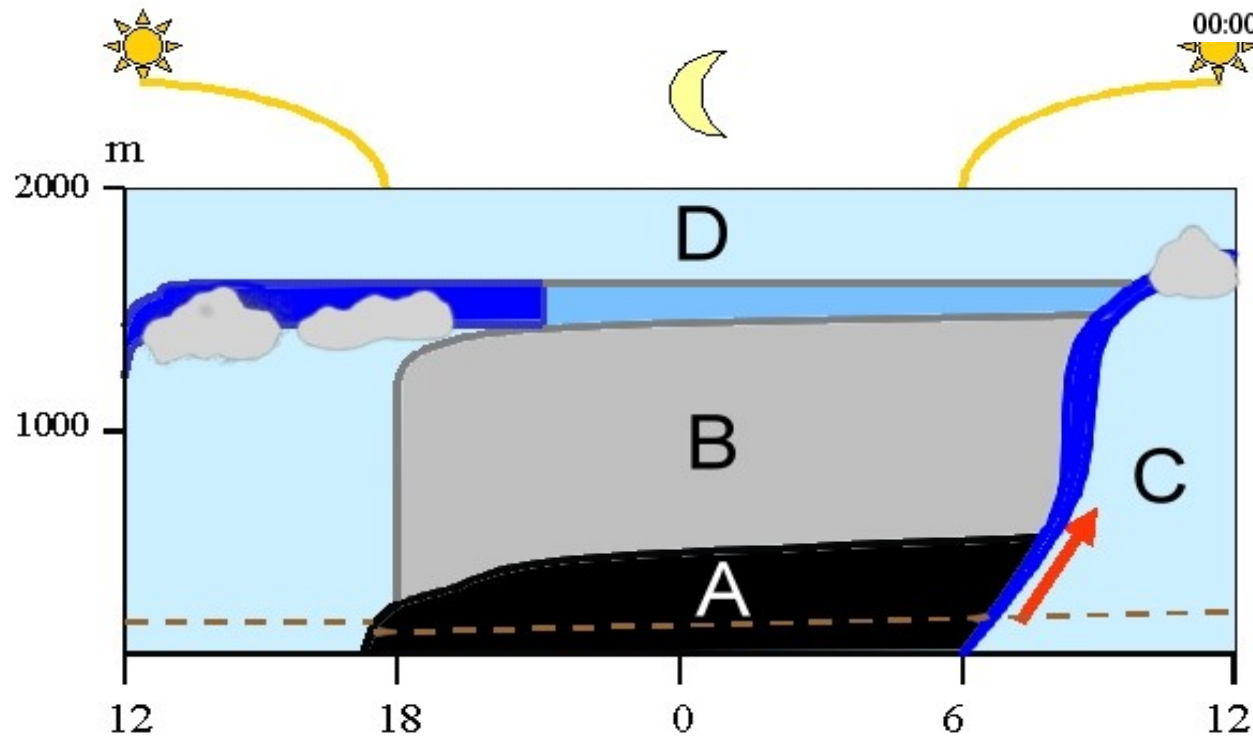
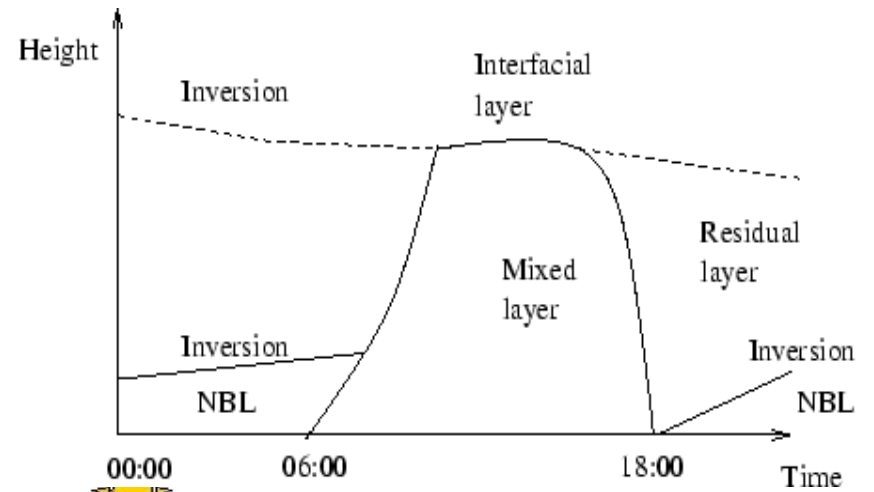
Figure 13. Time-averaged TKE budget terms (see abscissa description in panels a-d) calculated for the last hour of the simulations and normalized to the cloud top. Colour code as in Figure 4.

PBL and its interaction with the surface



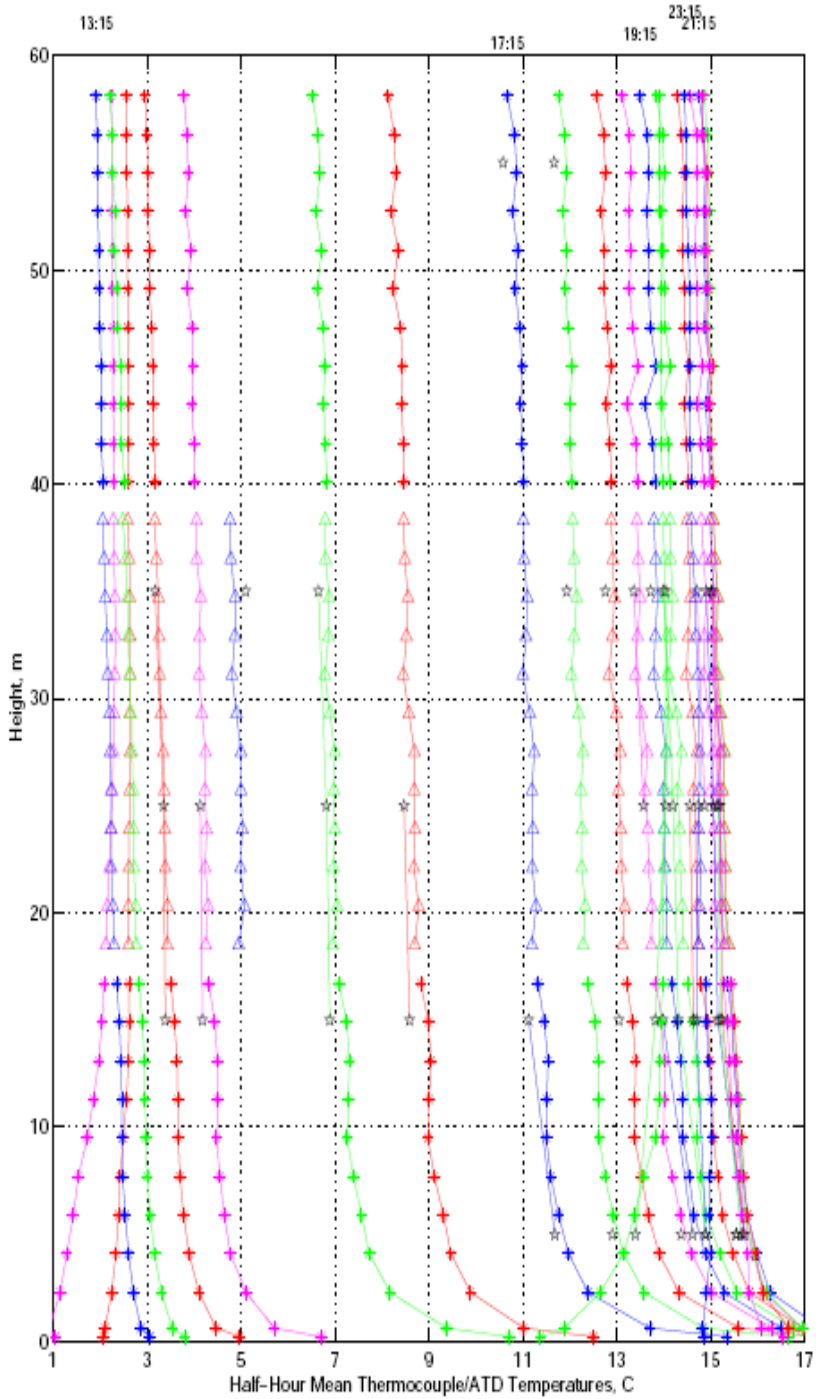


Diurnal cycle of PBL.



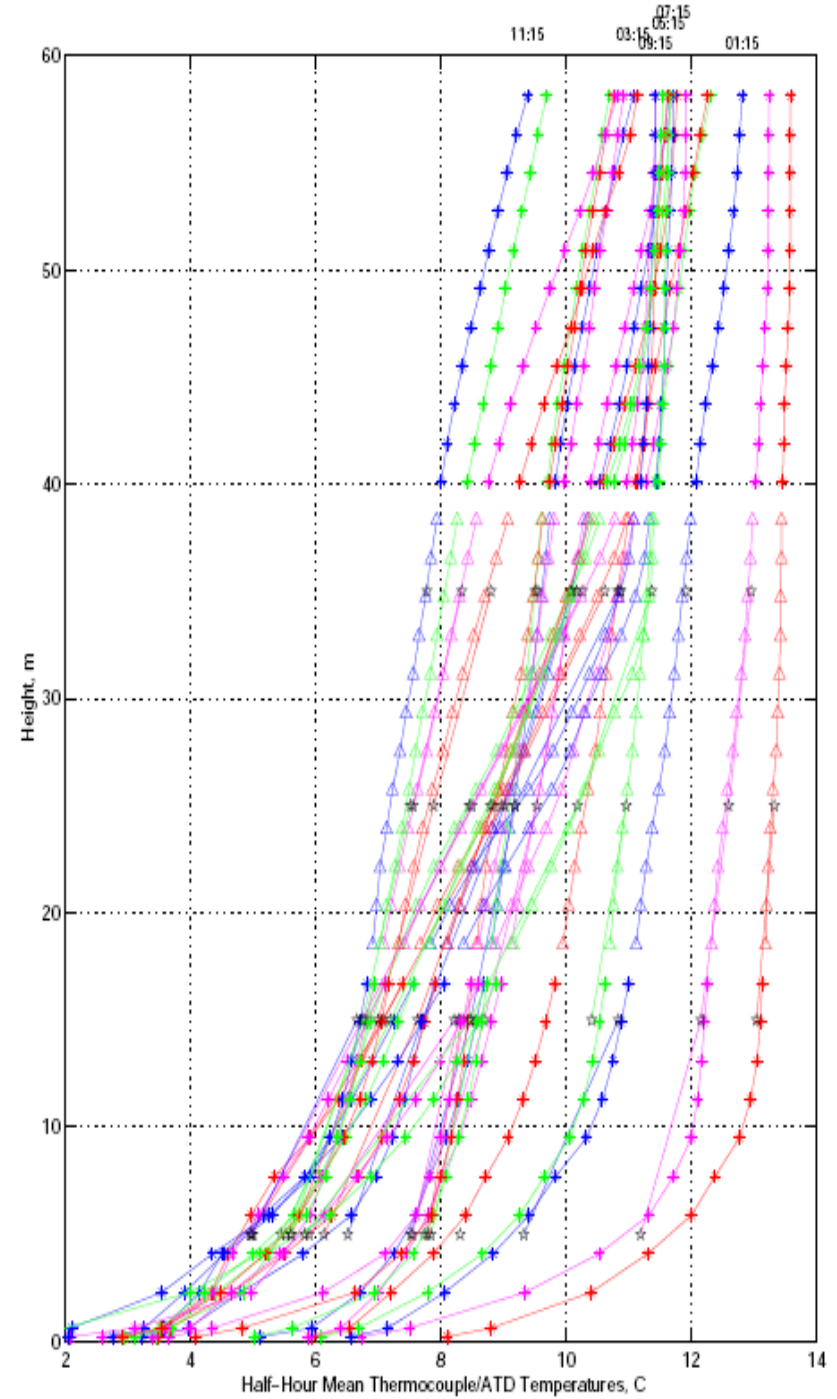
☆ = ATD Aspirated Data
10/04 12:00:00 - 10/04 23:59:59 UTC

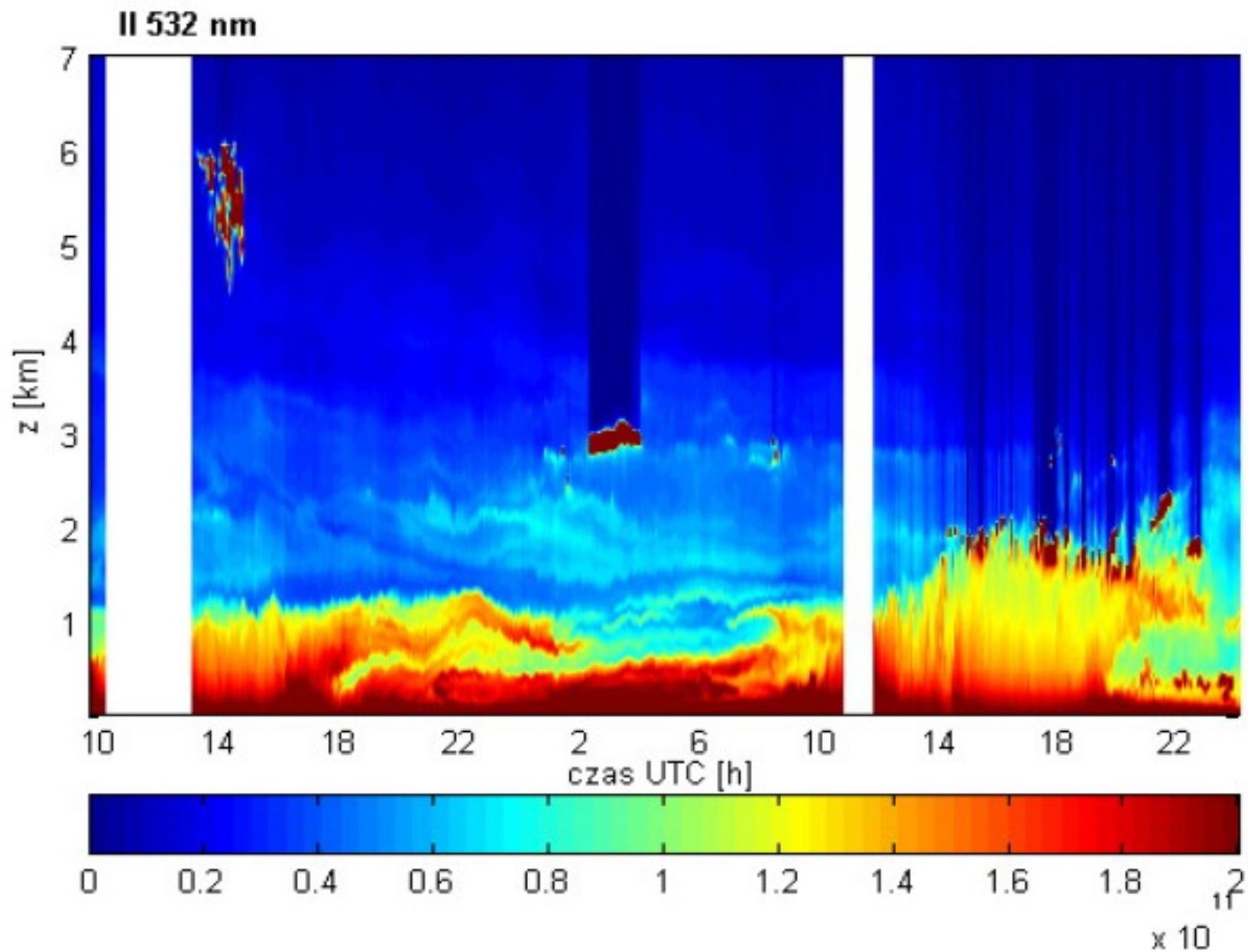
Script File: -seanfradlab\hvac\scpiplot_profilem
Spd - Date: 11-Dec-2020



☆ = ATD Aspirated Data
10/05 00:00:00 - 10/05 11:59:59 UTC

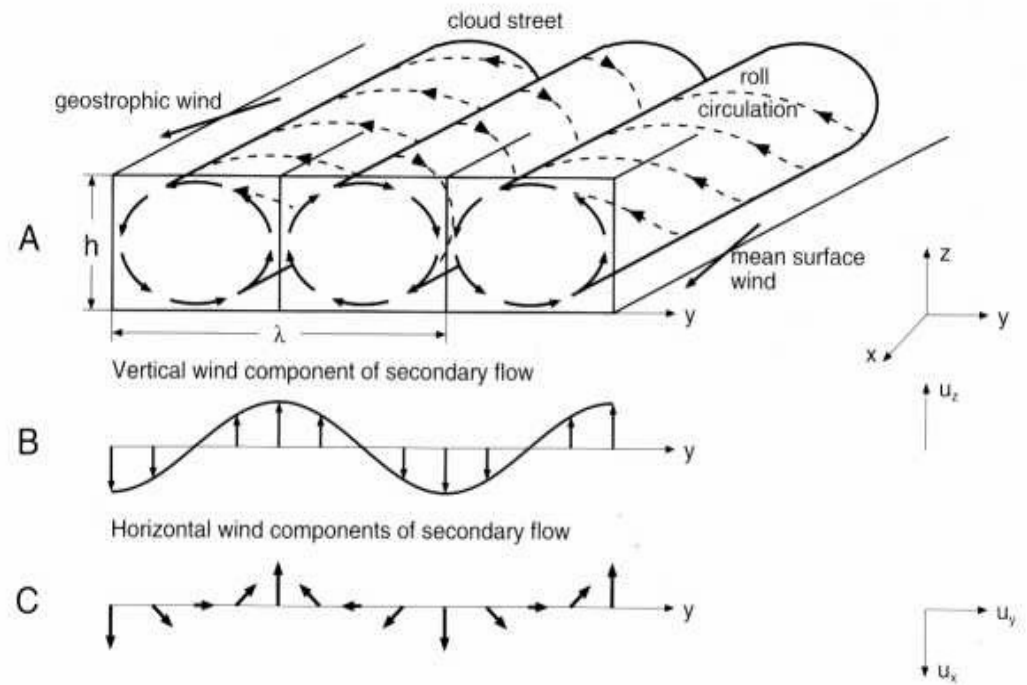
Script File: -seanfradlab\hvac\scpiplot_profilem
Spd - Date: 11-Dec-2020

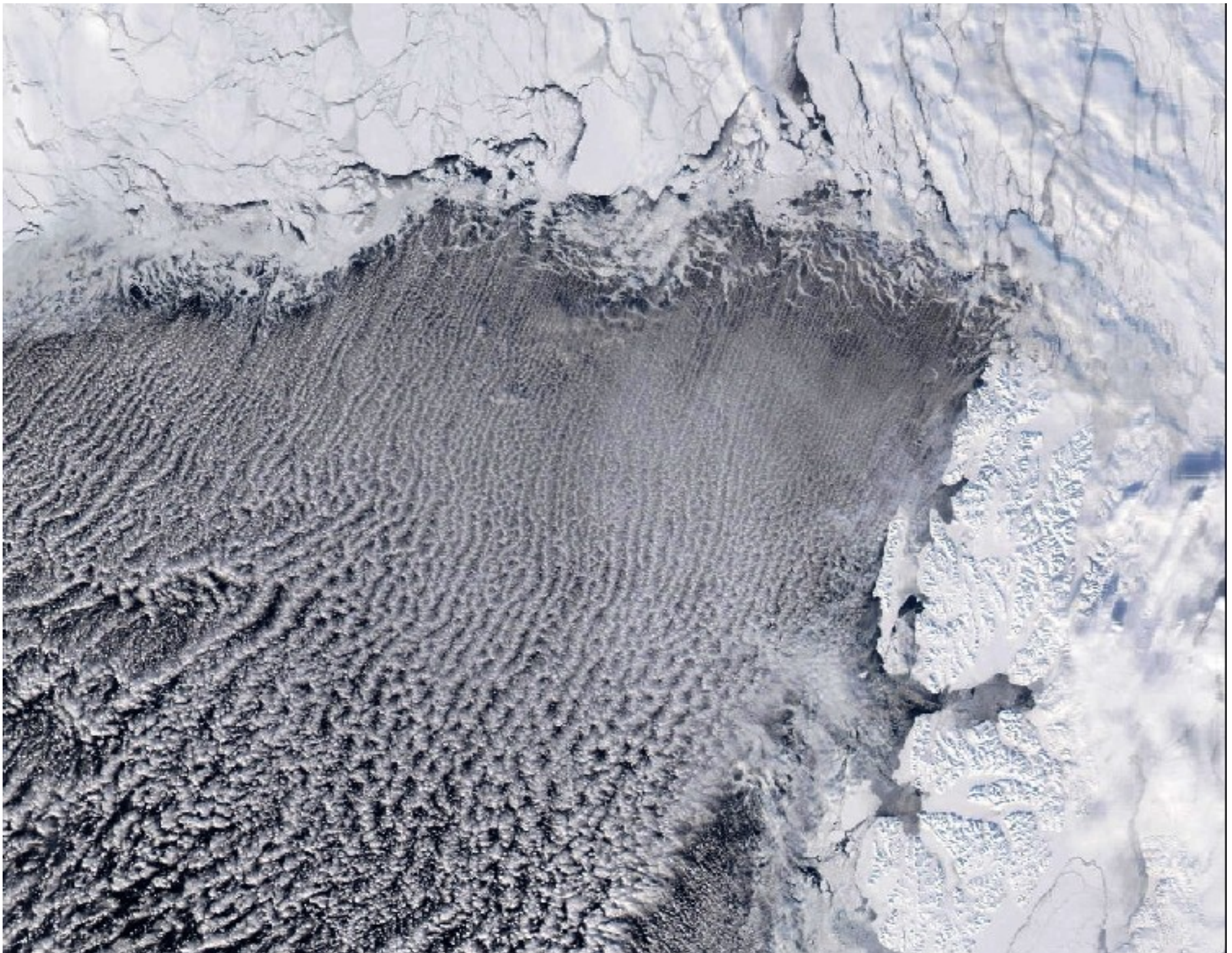




Lidar returns (532nm) in the atmospheric boundary layer allow to investigate its evolution. Notice that lidar signal are scattered by dust and cloud droplets,

Convective rolls:
organization of
convection.
Turbulence?
Coherent structures in
turbulence!





Convection rolls in cold air outbreak over a warm sea surface